International Journal of Environmental Sciences
ISSN: 2229-7359
Vol. 12 No. 1, 2026
https://theaspd.com/index.php

The Potential of Acacia Raddiana Bark as A Low-Cost Biosorbent for Removing Methylene Blue Dye From Aquous Solution

Agha Leila[1,2*], Cheriti Abdelkrim[1], Hacini Salih[2]
[1]Phytochemistry & Organic Synthesis Laboratory (POSL), Faculty of Medecine, Tahri Mohamed University Bechar, 08000, Algeria
[2]Depertement of Chemistry, Sciences Exacts Faculty, University Ahmed Ben Bella Oran1, Oran, 31000, Algeria

Received :15/03/2025 ***Accepted :10/02/2026*** ***Published :27/03/2026***

Abstract
The present study examines the potential of using Acacia raddiana bark as a sustainable, low-cost biosorbent for removing methylene blue (MB) dye from wastewater. Comprehensive characterization of the biosorbent was completed using FTIR, SEM-EDX, BET, XRD, and the pH point of zero charge (pHpzc) was determined. According to experiment, the equilibrium times of was found to be 100 min, with a maximum adsorption capacity of 9.128 mg/g. The optimum pH=10, and MB initial concentration =10 mg/L. The thermodynamic data revealed an endothermic mechanism adsorption (ΔH = 66.72 kJ/mol) and spontaneous process (ΔG = −0.77 kJ/mol), with adsorption efficiency gradually rising with temperature. The Langmuir model showed the strongest correlation (R^2 = 0.99), indicating monolayer adsorption with a maximum Langmuir adsorption capacity of 10.04 mg/g at 15 °C. The process follows a pseudo-second-order model (R^2 = 0.99). FTIR analysis confirmed the existence of functional groups (O–H, C=C), which are important binding sites involved in the process of MB biosorption. The material has an irregular, porous structure and a surface area of 5.617 m^2/g. On the whole, the findings suggest that Acacia raddiana bark is a promising natural sorbent for treating dye-polluted wastewater.
Key Words : *adsorption ; dye ; pH ; Acacia raddiana ; isotherm ; thermodynamics ; kinetic*

1.INTRODUCTION

Many nations face challenges related to industrial wastewater, which often contains high levels of pollutants. This pollution is primarily caused by various industries, most notably the dye industry, which produces large quantities of wastewater containing hazardous chemicals and nanomaterials (Afolalu et al., 2022) Dye-laden wastewater is among the most extensively studied categories of industrial effluents. Therefore, proper treatment is necessary before such wastewater can be discharged into the environment (Dutta et al., 2021). One of the major issues that has emerged with industrial expansion is the presence of dye pollutants in wastewater, which necessitates the development of effective biosorbents (Shanableh et al., 2023). Synthetic dyes are a major contributor to environmental pollution and are used in many sectors, including textiles, food processing, paints, the automotive industry and construction (Sarioz et al., 2024). The Textile Color Index states that 10,000-plus varieties of textile dyes are produced every year, with a total output of around 700,000 tons (Onuk et al., 2025). It is estimated that 10–15% of these dyes are discharged into ecosystems, and approximately 70% of them belong to the azo dye group (Periyasamy., 2024). There are three types of dyes: anionic, cationic, and non-ionic. Methylene blue, chemically defined as 3,7-bis (dimethylamino)-phenothiazin-5-ium chloride, is a positively charged thiazine dye that forms a stable water solution under ambient conditions. It is also stable in the presence of light and heat, and its complicated structure makes it difficult to break down (Sarojini et al., 2022). This cationic dye is widely applied to color cotton, silk, and linen fabrics. Despite its extensive use, MB dye poses several risks to human health, including breathing difficulties, edema, nausea, jaundice, and even cell lysis (Kumari et al., 2025). Bio-resistant pollutants such as methylene blue (MB) are not efficiently eliminated by conventional biological, chemical or physical treatment methods due to their persistence and the high cost associated with their removal. These methods include ionic exchange, photocatalysis, electrochemical coagulation, membrane filtration and activated sludge processes (Abdel Azim et al., 2024). Among the various treatment approaches, adsorption onto solid materials considered a highly effective physicochemical process has been extensively studied (Khan et al., 2022). Adsorption is a scalable and adaptable technique that can be implemented in both extensive and local water purification systems. Its advantages include potential renewability, operational simplicity, and selective pollutant removal. Its rapid kinetics, compatibility with various treatment techniques, and lack of hazardous residues enhance its attractiveness as an effective and sustainable method for wastewater treatment (Nipa et al., 2023). It is an environmentally friendly wastewater treatment choice because it works with a variety of treatment techniques and produces no harmful. The purpose of this

study is to assess a biosorbent derived from a natural resource: the bark of the endemic *Acacia raddiana* species found in southwest Algeria. The objective is to demonstrate this natural substance's efficacy as a biosorbent and its potential as a cost-effective substitute for methylene blue removal from aqueous systems. This study investigates the effects of several variables, such as the biosorbent dose, initial dye concentration, pH level, exposure duration, and temperature, on the effectiveness of methylene blue removal. The experimental results were analyzed to investigate the adsorption equilibrium and the thermodynamic and kinetic characteristics.

2. MATERIAL AND METHODS

2.1. Preparation of adsorbent

For four days, the biological material was dried outside and in the dark. Then, the sample was subjected to oven drying at 50°C for a duration of one hour. After that, it is ground with a FRITSCH-type grinder to make an uniform material with a small grain size for lab studies. The procedure involved washing the ground material by bringing it into contact with an appropriate quantity of distilled water. A magnetic stirrer was used to stir the suspension for 24 hours; this operation removed all the grinding residue. The material was dried again at 50°C until its mass remained the same. Finally, the particles intended for adsorption experiments were separated mechanically using a 0.5 mm size, and the prepared biomass was stored in a glass container.

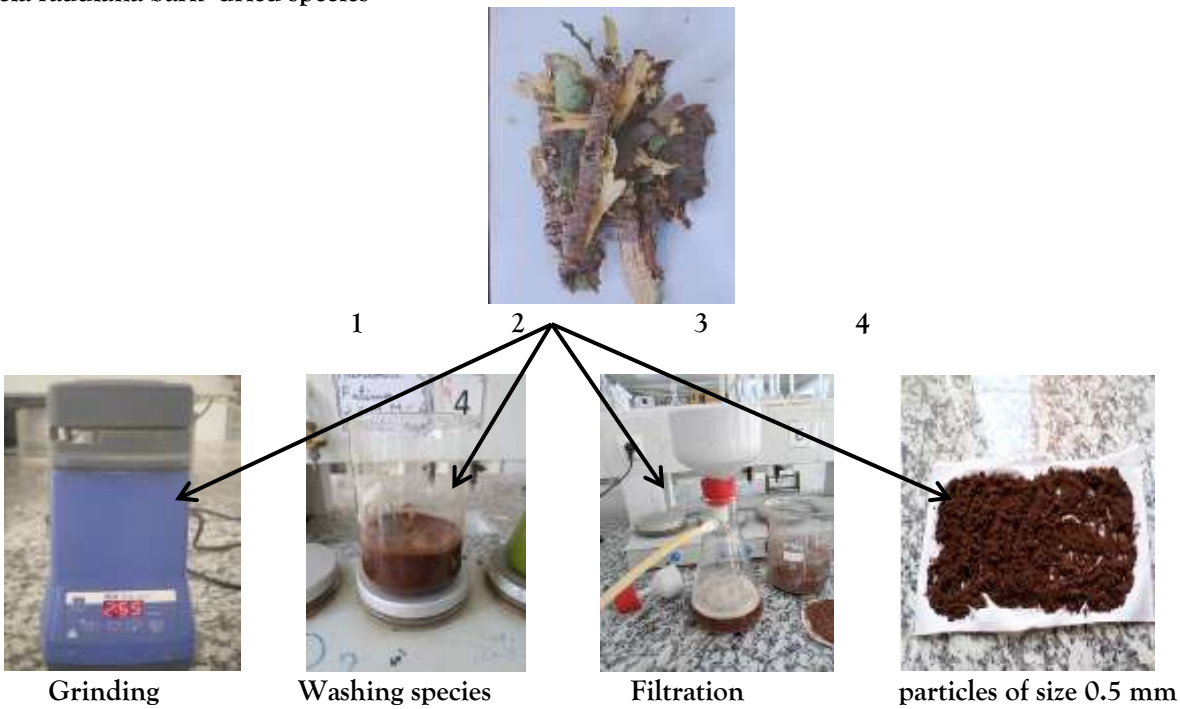

Fig 1. Adsorbent preparation procedure.

2.2. Characterization of *Acacia raddiana* bark

2.2.1. Fourier Transform Infrared Spectroscopy analysis

Characterization of the outer layer binding sites of the adsorbent was carried out using FTIR analysis with an Agilent Cary 630 model, operating at ambient temperature over a frequency range of 4000–400 cm^{-1}. Using Brunauer-Emmett-Teller (BET) analysis on a Micromeritics ASAP 2020 plus instrument, we found out the samples' superficial area and pore size distribution.

2.2.2. Surface morphology analysis

The SEM analysis offers insightful information about the surface features and structural characteristics of *Acacia raddiana* bark biosorbent for the processes of adsorption. The surface morphology and elemental composition were analyzed using a field emission scanning electron microscope (ThermoScientific Scios 2 DualBeam) coupled with energy-dispersive X-ray spectroscopy (EDX).

2.2.3. X-ray diffraction (XRD) analysis

A crucial piece of equipment for determining whether biosorbents are crystalline or amorphous is X-ray diffraction (XRD). The crystallinity of the *Acacia raddiana* bark was investigated using a powder X-ray diffractometer (Bruker D8 Advance A25) with an X-ray wavelength of 1.54 Å.

2.2.4. Point of zero charge (pHpzc) determination

The determination of the pH point of zero charge (pH_{ZPC}) was performed using the "pH drift method" (pHdrift method), adapted to account for the adsorption capacity of the bioadsorbent. This was accomplished by preparing six NaCl blank solutions with a pH range of 2 to 12 and a concentration of 0.01 mol/L that were adjusted using either 0.1 M HCl or 0.1 M NaOH. 50 ml of each of these solutions was then mixed with 0.1 g of bioadsorbent. The resulting suspensions were maintained under agitation (300 rpm) for 72 hours at room temperature (25±2°C). The pH_{PZC} was determined from the intersection of ΔpH (= pHf - pHi) curve with pHi axis (Kifuani et al., **2018**).

2.2.5. Preparation of the stock solution of the "methylene blue" dye

Methylene blue was designated as an illustrative example for an organic colorant due to its extensive application in laboratory settings and its efficacy in dyeing silk, cotton, and wood, as well as its accessibility and toxicity (Rana et al. **2021**).To prepare the methylene blue stock solution, fifty milligrams of the colorant were mixed with one liter of distilled water. This made a solution with a concentration of 50 mg/L. After stirring it well, a dark blue solution that was uniform was made.

2.3. Adsorption studies

To establish the best operational parameters for improving the sorption of methylene blue by *Acacia raddiana* bark biomass, an adsorption study was performed. Five factors were examined to assess their impact on MB removal: exposure time (min), solution pH, adsorbent dosage (g/L), MB concentration (mg/L), and temperature of reaction mixture. The experiment started with an evaluation of the contact time variable by analyzing samples subjected to shaking periods of 5, 10, 20, 40, 50, 60, 80, 100, 120, and 150 minutes in flasks of 100 ml MB mixture (50 mg/L) at pH 5, with a biosorbent/ biosorbate dosage ratio of 5g/L, maintained at 15°C. Under the same setups, three simples were filled with 100 ml of MB solution (50 mg/L), pH values of 2, 5, and 10 were set by adding 0.1 N of both hydrochloric acid and sodium hydroxide solutions. Each solution was shaken for between 5 and 150 minutes. The influence of dosage was examined for a range of adsorbent concentrations of 1, 2, 5, 8 and 10 g/L per 100 mL of an MB solution having a concentration of 50 mg per liter, maintaining consistent pH and adsorbent dosage conditions. Subsequently, Different MB concentrations (10, 20, 50, and 80 mg/L) were tested to assess the concentration effect, and temperature influence was investigated at 15, 25, 30, 35 and 60°C using 100 Ml MB solutions of 50 mg/L with a biomass concentration of 5 g/L at pH 5 for 60 minutes. Furthermore, tests for adsorption isotherms, thermodynamics, and kinetics were carried out. After shaking, the samples were allowed to rest, and 5 mL aliquots were taken, centrifuged, and analyzed with a SPECORD 50 PLUS spectrophotometer at 665 nm, as indicated in Equation (2) (Manera et al., **2019**), shows how to find the adsorption capacity (qe), which is the quantity of methylene blue that a unit mass of *Acacia raddiana* bark can absorb at equilibrium.

$$qe\ (mg/g) = \frac{C0 - Ce}{m} \times V \qquad (1)$$

The parameter qe denotes the quantity of MB Adsorbed to mass of adsorbing material (mg/g); C_0 and Ce correspond to the starting and at equilibrium of MB concentrations (mg/L), respectively; V is the aqueous solution volume (L), and m refers to the dry adsorbent mass (g).

3. RESULTS AND DISCUSSION

3.1. Characterization of *Acacia raddiana* bark

The FTIR spectrum analysis of the biomass *Acacia raddiana* bark in Figure 2 shows several functional groups that are directly associated with the biosorbent's ability to extract methylene blue from solutions. In particular, The broad peak at 3334 cm^{-1} corresponds to O–H stretching vibrations, indicating the presence of hydroxyl groups (Hamzah et al., **2023**) and the presence of free and bound hydroxyl groups and functional groups such as -COOH and -COH. And the peaks identified at 2922 and 2849 cm^{-1} correspond to the asymmetric and symmetric C–H stretching vibrations of CH and CH_2 groups in the methyl and methylene groups of lignin molecules found in cellulose and hemicellulose constituents (Kassahun et al., **2022**; Sen et al., **2024**). Additionally, The Spectral maximum at 1617 cm^{-1} suggest the stretching vibration of the C=C bond the manifestation of unsaturated olefinic linkages in alkenes and aromatic compounds, stretching vibrations of C = O in ketones and C=C bonds in carbonyl groups (Nursiah et al., **2023**). The peak at 1448 cm^{-1} confirms the existence of a benzene ring [Sen et al., **2024**; Kumari et al., **2023**). The Spectral maximum at 1015 cm^{-1} reveals the C–O groups (Mohamed et al., **2022**).

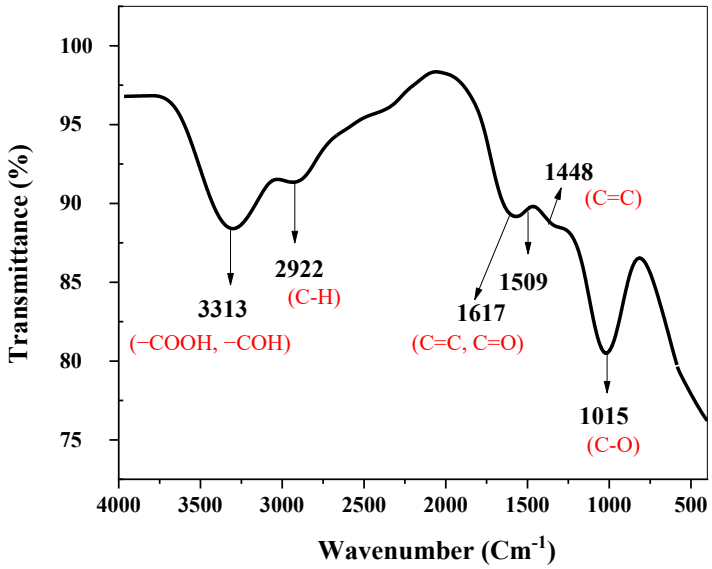

Fig 2. FTIR spectrum

The XRD analysis of the biosorbent derived from *Acacia raddiana* indicates predominantly amorphous characteristics. The peak observed between 2θ 15 and 24° (Figure 3.a) corresponds to the amorphous structure of cellulose, hemicellulose, and lignin, the main components of plant-based biosorbents (Singh et al., 2020; Montoya-Escobar et al., 2022). The low crystallinity appears in the absence of sharp crystalline peaks. The peak detected at 2θ 38° could be explained by minute amounts of inorganic elements like minerals based on calcium. The adsorption-desorption isotherm of nitrogen (N_2) on *Acacia raddiana* biomass is shown in Figure 3.b and has a typical type II isotherm. *Acacia raddiana* organic matter has a surface area of 5.617 m^2/g, a total pore volume of 0.00697 cm^3/g, and a pore diameter of 5.49 nm, all of which are indicative of mesoporous properties, according to BET analysis.

The SEM examination of the studied biomass *Acacia raddiana* bark depicted in Figure 3.c, based on the image, showed a denser surface morphology and highly irregular and porous features that can facilitate effective pollutant adsorption (Wang et al., 2020). The EDX spectrum confirms the dominance of carbon and oxygen, the key elements instrumental in the adsorption process, with oxygen being of particular significance because it forms hydroxyl groups that assist methylene blue adsorption through hydrogen bonding (Dimbo et al., 2024). Calcium (Ca) is apresent with an important mass ratio. Several trace elements were detected in the EDX spectra of the *Acacia raddiana* biomass, including chlorine (Cl), potassium (K), sulfur (S), magnesium (Mg), aluminum (Al), and silicon (Si).

The surface characterization of *Acacia raddiana* biomass showed that it has a pHpzc value of 7.1 (figure 3.d), which means that at this pH, the material is electrically neutral, and its surface behavior depends on the pH of the surrounding medium. If the pH < 7.1, protonation of the surface functional groups makes the surface positively charged. As a result of the prevalence of H^+ ions, which is beneficial for the adsorption of negatively charged pollutants. If the pH > 7.1, a negatively charged surface is the results of deprotonation due to the prevalence of OH^- ions, enabling the adsorption of positively charged pollutants like MB dye (Gamboa et al., 2024).

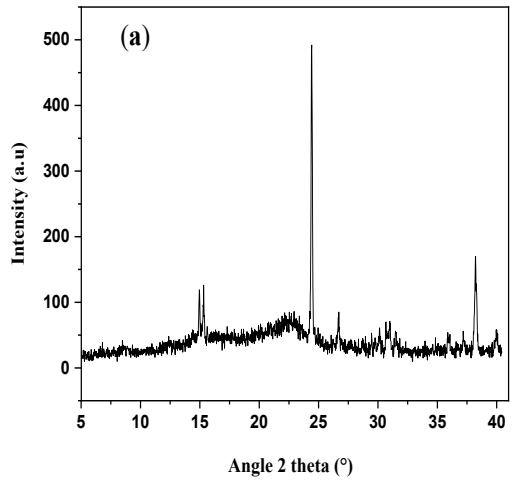

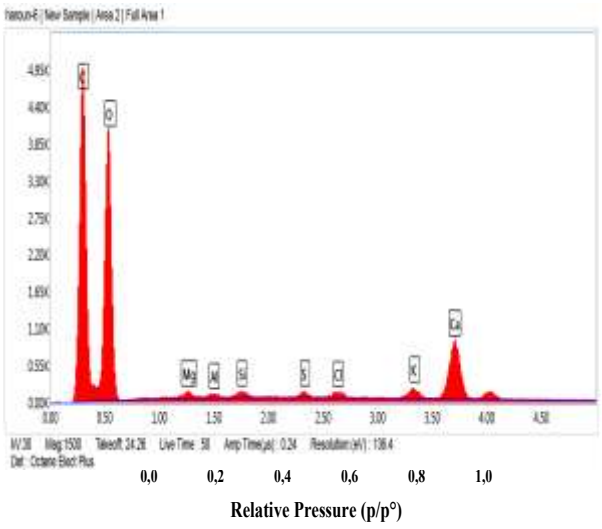

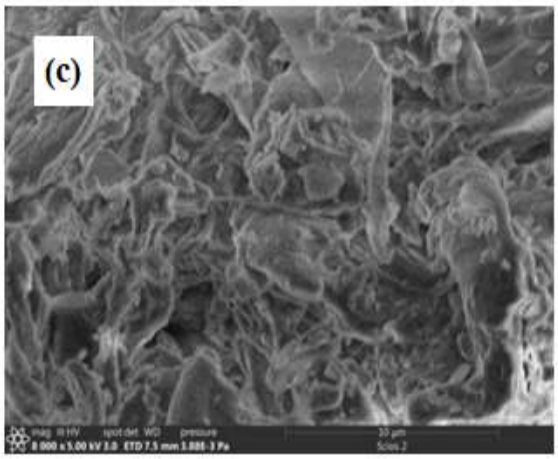

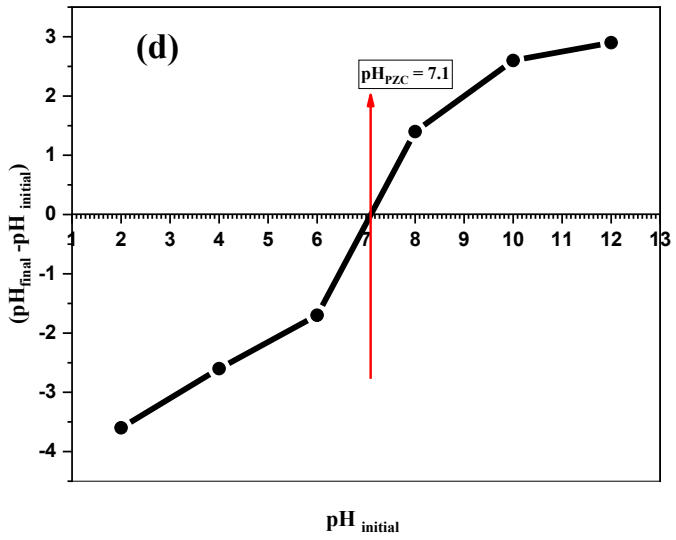

Fig 3. **(a)** DRX pattern, **(b)** N_2 adsorption-desorption isotherms, **(c)** SEM–EDX, **(d)** pH_{PZC}

3.2. Adsorption Optimization

3.2.1. The Effect of Interaction Time

Figure 4 presents the variation of the contact time for MB removal on the *Acacia raddiana* biomass ; studying exposure time is vital for establishing the suitable period required to attain the equilibrium contact time for MB adsorption. During the procedure, referring to the figure below, colorant was eliminated from the solution with qe = 7.21 mg/g in the first 10 min. The equilibrium plateau is reached at the end of 100 min for a qe = 9.128 mg/g. Thereafter, the adsorption rate is nearly constant up to 150 minutes. This aligns with earlier research showing evidence that effective MB removal is achieved with an optimal contact time of about 60 minutes (Ashraf et al., **2024**) and 90 minutes (Asgari et al., **2024**). There are many surface sites where MB can attach, which explains the quick initial uptake. There are many surface sites where MB can attach, which explains the quick initial uptake. However, over time, the repulsive forces between the adsorbed binding sites make it more difficult to fill the remaining active sites. This reduces its ability to remove MB (Salameh et al., **2025**).

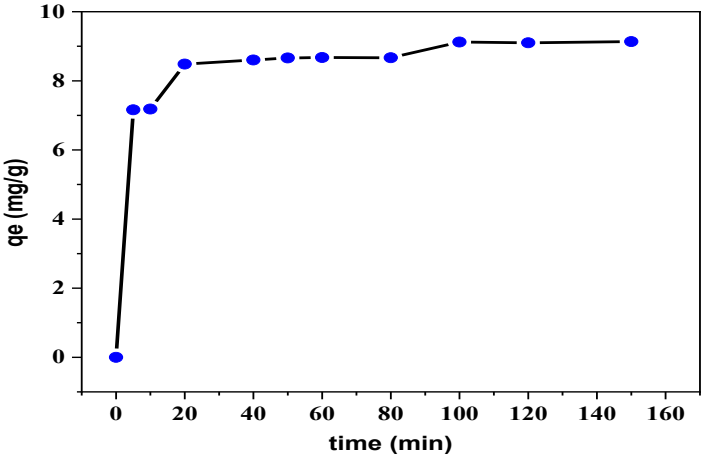

Fig 4. The impact of exposure time on retention of MB by *Acacia raddiana* biomass C_0 = 50 mg/L; T = 15±2 °C; r = 5g/L; pH = 5

3.2.2. The Effect of pH of the solution

Methylene blue (MB) is a cationic dye that produces positive ions when dissolved in water (Jaramillo-Fierro et al., **2024**). The study revealing adsorption capacities of 8.8, 9.2, and 9.5 mg/g onto *Acacia raddiana* biomass at the pH values of 2, 5, and 10, respectively. In the figure 5, as the pH increases, the adsorbent's surface will have more negatively charged groups. Consequently, cationic dyes will adhere to it more readily. This phenomenon arises due to the attenuation of repelling forces between dye cations and the outer layer of the adsorbent molecules (Onuk et al., **2025**). The highest amount of MB removal is observed when the pH rises to 10. In acidic environments (pH < 6), hydronium ions (H_3O^+) compete for adsorption sites on the adsorbent particles. Consequently, MB adsorption is less efficient because fewer active sites are available. Additionally, the adsorption method is less effective in acidic environments because the repelling forces between the MB constituent and the adsorbent particles are stronger (Haleem et al., **2023**).

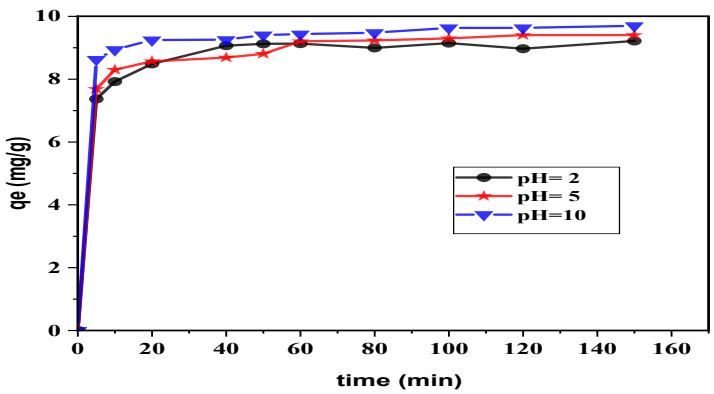

Fig 5. The impact of pH on the retention of MB by biomass *Acacia raddiana*. C_0 = 50 mg/L; T = 15±2 °C; r = 5g/L

3.2.3. The Effect of MB Initial Concentration

To study the effect of the initial MB concentration on *Acacia raddiana* bark, tests were carried out using MB molarities of 10, 20, 50,80 and 100 mg/L as the starting point. All other parameters were kept constant. Generally, the higher the initial MB molarity, the higher the adsorption curve. Figure 6 illustrates how the methylene blue eradication efficiency for *Acacia raddiana* bark rises with concentration from 10 to 100 mg/L, with qe rising from 8.2 to 9.85 mg/g. This is explained by the fact that MB molecules in the solution attach to open locations on the adsorbent surface, which fill up as the molarity rises (Bih et al., 2025).

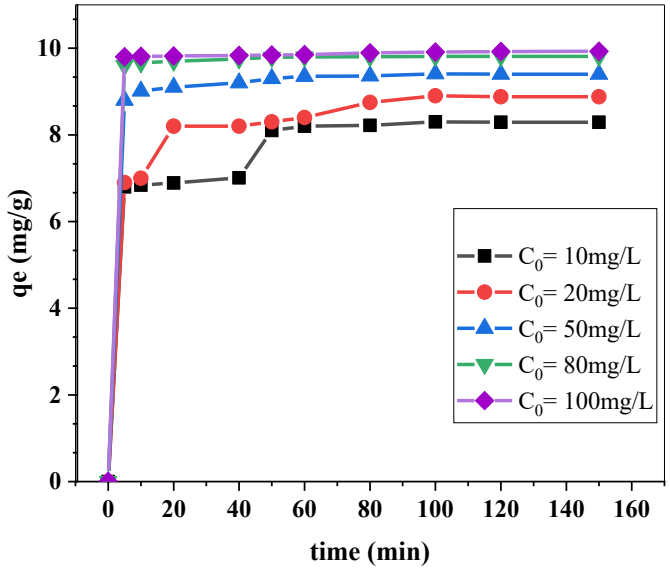

Fig 6. The effect of the initial concentration on the retention of methylene blue by the biomass of *Acacia Raddiana* T= 15±2 °C; r = 5g/L; pH = 5

3.2.4. The Effect of Adsorbent Dosage

The adsorption tests based on biosorbent mass were conducted in a discontinuous system. Doses of *Acacia raddiana* biomass at 1, 2, 5, 8, and 10 g/L were used while all other parameters were held constant. The curves in Figure 7, demonstrate that as the adsorbent dose increases, so does the adsorption of MB particles, with the amount removed increasing from 3.41 mg/g to 9.67 mg/g at 100 minutes of exposure time. Results showed a positive correlation between adsorbent dose and removal efficiency, indicating that the efficiency improves as the adsorbent amount increases. This behavior results from the presence of additional adsorption sites and an expanded surface area facilitating adsorption, which increases the attractive forces between the biomass's negative charges and MB's positive charges, thereby increasing the adsorption capacity (Cai et al., 2024).

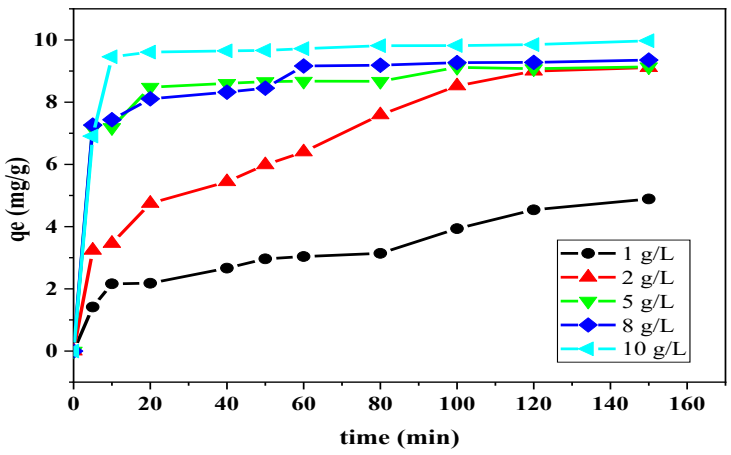

Fig 7. The effect of adsorption dosage on methylene blue retention by *Acacia raddiana* biomass C_0= 50 mg/l, T=15±2 °C, pH = 5

3.2.5. The Effect Of Temperature On Adsorption:

The effect of temperature on the adsorption of methylene blue (MB) was investigated by preparing dye solutions at a pH of 5 and maintaining them at specific temperatures in a water bath: 15, 25, 30, 35, and 60°C. As exhibited in figure 8, greater adsorption is preferred at higher temperatures, as the equilibrium adsorption ability (qe) improved from 8.93 mg/g at 15°C to 9.92 mg/g at 60°C. As temperature rises, the movement of retained molecules through the surrounding boundary zone and into the adsorptive material accelerates as a result of the lowered viscosity of the surrounding solution (Cheruiyot et al., **2019**).

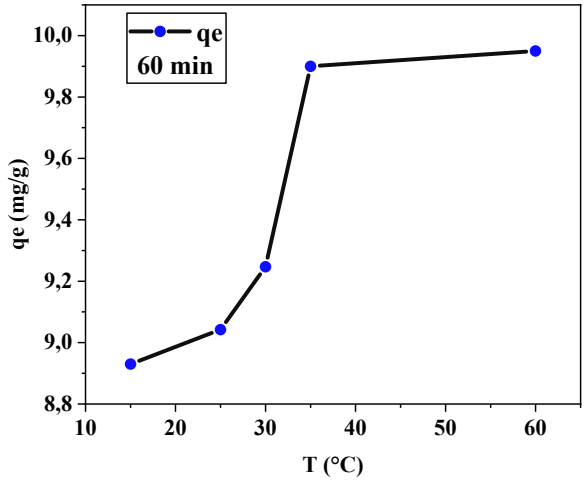

Fig 8 . Effect of temperature on the retention of MB by *Acacia raddiana* biomass
C_0 = 50 mg/L; r = 5 g/L; pH = 5

3.3. Adsorption thermodynamics

A study was conducted in order to describe the thermo-energetic properties of MB sorption onto *Acacia raddiana* bark by quantifying the variations in Gibbs free energy (ΔG, kJ/mol), entropy (ΔS, J/mol.K), and enthalpy (ΔH, kJ/mol), by applying these three formulas to determine the thermo-energetic parameters (Kumari et al., **2025**):

$\Delta G° = \Delta H° - T \times \Delta S°$ (2)

$\Delta G° = - RT \ln K_d$ (3)

$K_d = \frac{qe}{Ce}$ (4)

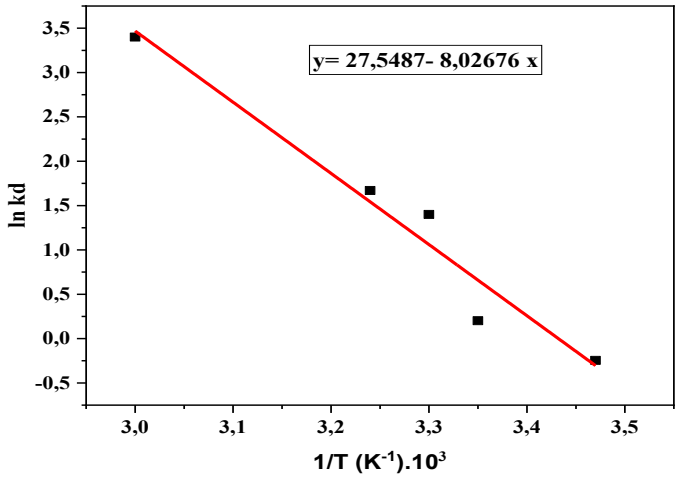

Fig 9. The determination of thermodynamics parameters of adsorption of MB

Table 1. Thermodynamics Parameters for the Adsorption of MB onto *Acacia raddiana* bark

	ΔG (kJ/mol)				ΔS (J/mol)	ΔH (kJ/mol)
T° (K)	288	298	303	308	333	

MB	-0.77	-1.52	-2.66	-3.18	-9.54	229	66.72

This finding is illustrated in Figure 9 and Table 1. The negative free energy values (ΔG) demonstrate that adsorption is spontaneous and that this process becomes more spontaneous at elevated temperatures, as evidenced by the decrease in ΔG° values with increasing temperature (Bhavyasree et al., **2021**). The ΔH° value was 66.72 kJ/mol. A positive enthalpy value confirms that the adsorption of MB dye onto Acacia raddiana bark is endothermic. Meanwhile, the positive ΔS° (299 J/mol K) indicates increased molecular disorder where the solid adsorbent comes into contact with the solution. This increased randomness at the adsorbent's binding locus further confirms the spontaneity of the process (Khairnar et al., **2020**, Yang et al., **2024**).

3.4. Adsorption Isotherms

The use of adsorption isotherms helps refine the design of adsorption systems and increase their efficiency. Multiple isotherm representation is typically stated to describe the equilibrium relation of adsorbent/adsorbate (Farghali et al., **2020**). Among the most frequently employed adsorption isotherm models are those of Langmuir, Freundlich and Temkin. The present research evaluated equilibrium adsorption isotherms for varying initial MB concentrations (10, 20, 50, 80 and 100 mg/L) under fixed parameters (pH 5, contact time 60 min, adsorbent dose 5 g/L at 15±2 °C).

3.4.1. Isotherm of Langmuir

The Langmuir model is suitable for systems in which adsorption occurs as a monolayer on surfaces with a limited number of unique sites. This theory assumes homogeneous and evenly distributed adsorption. Linearized form of the Langmuir's isotherm is given by the subsequent equation:

$$\frac{Ce}{qe} = \frac{1}{KL.\ q\,max} + \frac{Ce}{q\,max} \quad (5)$$

The determination of the equilibrium parameters qmax and KL of the equation is achieved by plotting $\frac{Ce}{qe}$ as a function of Ce. This results in a line with a slope of $\frac{1}{qmax}$ and an ordinate at the origin of $\frac{1}{KL.qmax}$.

Where: q_m refers to the peak sorption ability (mg/g), q_e stands for the steady-state ability corresponding to a finished mono-layer (mg/g), K_L is the stable linked to site-specific affinity and interaction energy (L/mg) and Ce: indicates the steady-state molarity (mg/L) (Ewis et al., **2022**).

3.4.2. Isotherm of Freundlich

The Freundlich isotherm is predicated on the spiculation that the adsorption is sevral-layer suggests a mixed nature of the adsorbent surface. The following relationships can be used to express this:

$$qe = K_f\ Ce^{1/n} \quad (6)$$

$$\ln qe = \ln K_f + \frac{1}{n} \ln Ce \quad (7)$$

The graphical representation of ln (qe) as a function of ln (Ce) is represented by a steering line. The coefficient of 1/n is initially ln (K_f) Where K_f refers to adsorption ability (mg/g) and $\frac{1}{n}$ is an empirical index that describes adsorption amplitude; values in the range of 0 to 1 reflect positive adsorption behavior (Vigdorowitsch et al., **2021**).

3.4.3. Isotherm of Temkin

According to the Temkin isotherm, adsorption occurs on both high-energy and non-equivalent locus of the adsorbent external layer, where the most energetic sites dominate the adsorption process (Javed et al., **2022**). The Temkin isotherm presumes an equal adsorption energy dispersion (up to a defined maximum), determined by plotting the equilibrium adsorption capacity (qe) against ln Ce ; its non-linear form is shown in Equation (9).

$$qe = B \ln(ACe) \quad (8)$$

$$qe = B \ln A + B \ln Ce \quad (9)$$

Where: B represents the adsorbent heat (J/mol). A denotes the steady-state constant related to the maximum adsorption energy. Ce denotes the steady-state molarity of MB (mg/L), and qe is the quantity of MB sorbed per gram of adsorbent at steady-state (mg/g).

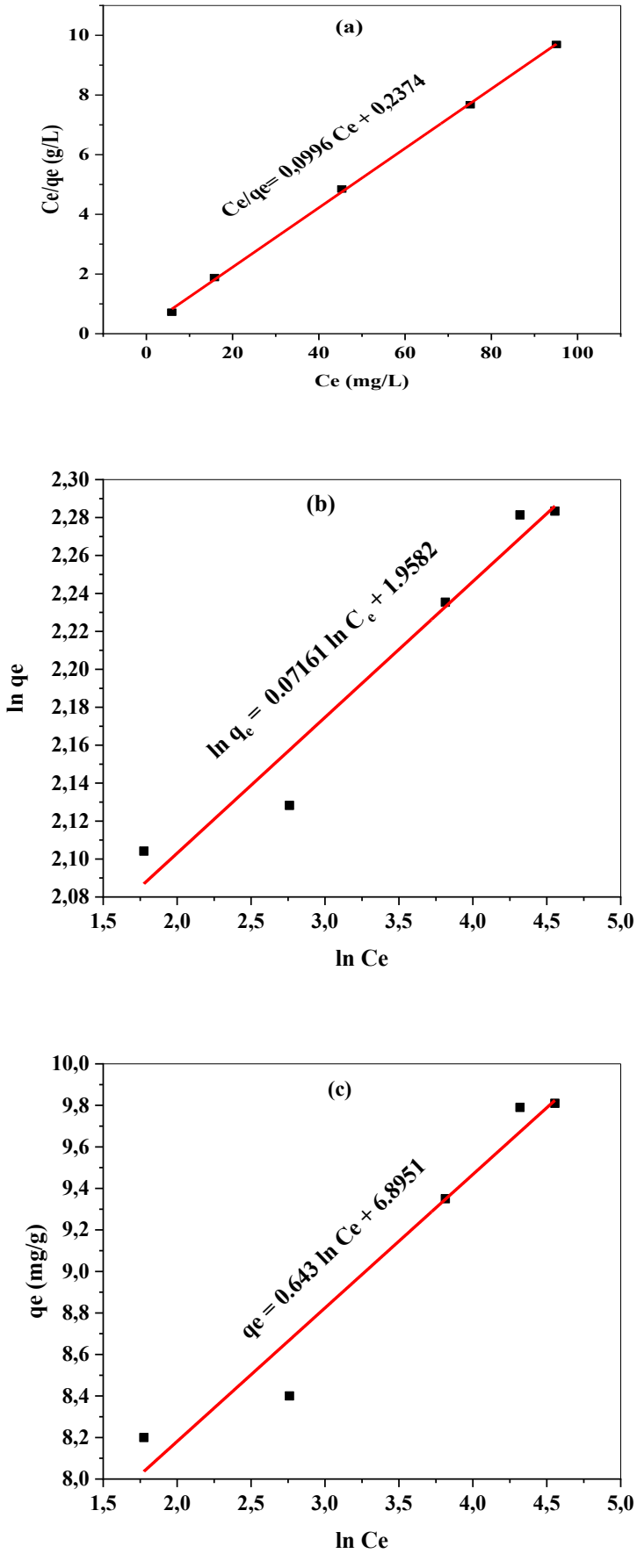

Fig 10. Linear isotherm models of MB adsorption onto *Acacia raddiana* bark : **a** Langmuir, **b** Freundlich, **c** Temkin

Table 2. Isotherm models' parameters for the adsorption of the BM onto *Acacia raddiana* bark

Model	Parameter	Values	R^2
Freundlich	K_f (mg/g)(L/mg)$^{1/n}$	7.08	0.954
	1/n	0.071	
Langmuir	K_L (L/mg)	0.42	0.999
	q_{max} (mg/g)	10.04	
	R_L	0.023	
Temkin	B (J/mol)	0.643	0.951
	A (L/mg)	45.25	

Table 2 shows the calculated constants corresponding to the Langmuir, Freundlich, and Temkin adsorption types. Based on the experimental data for the three models and the R^2 coefficient values, Langmuir's model appears to best explain how MB sticks to *Acacia raddiana* bark biomass (R^2 = 0.99) with maximum adsorption capacity (q_{max}) = 10.04 mg/g . The Langmuir constants with the low value K_L = 0.42 L/mg and the separation factor R_L = 0.023 in the range of $0 < R_L < 1$ both confirm that the adsorption is favorable (El-Nemr et al., **2023**). This strongly suggests that MB is adsorbed onto the adsorbent in a single layer. The binding sites were homogeneously dispersed across the adsorbent surface, displaying uniform affinity for each colorant molecule. This implies that each active site is occupied by a single colorant molecule (De Oliveira et al., **2023**). Compared to Langmuir, the Freundlich (R^2=0.954) and Temkin (R^2=0.951) models are less appropriate for explaining this particular system, despite both having comparatively high correlation coefficients. The weaker fit for the Freundlich model suggests that multilayer development or a highly heterogeneous surface are not the main sites of adsorption. Similarly, the Temkin isotherm's lower R^2, which takes into consideration the impact of indirect adsorbent-adsorbate interactions, indicates that the heat of adsorption does not drop linearly with coverage as the model predicts.

3.5. Adsorption Kinetics

The adsorption flux is expressed as the variation between the quantity of adsorbate retained at duration (qt) and the steady-state adsorption amount (qe), according to the basic equation that characterizes the movement of materials between two phases. All transfer resistances are found at the liquid-solid interface, where material transfer determines the adsorption phenomenon's kinetics (Ezzati et al., **2024**). In the current endeavor, pollutant sorption kinetics was tested through the pseudo-first-order, pseudo-second-order, and intraparticle diffusion models, whose nonlinear expressions are given as follows:

This model helps to elucidate the adsorption ratio and how it relates to the adsorbent's capacity for adsorption. Equation 10 represents the pseudo-first-order kinetic model.

$$q_t = qe\ (1 - e^{-k1t}) \qquad (10)$$

Here, k_1 refers to the pseudo-first-order kinetic rate constant [min^{-1}]; qe and qt are the adsorption ability (mg/g) at time t and at steady-state, respectively (Al-Harby et al., **2021**).

$$q_t = \frac{qe^2 k_2\, t}{1 + q_e\, k_2\, t} \qquad (11)$$

In this expression, k_2 is the rate constant for second-order kinetics [g/mg.min], while qt and qe correspond to the adsorption ability (mg/g) at time tand steady-state (Kucuk., **2024**).

$$q_t = k_{int}\, t^{1/2} \qquad (12)$$

$$q_t = k\, t^{1/2} + C \qquad (13)$$

Where k_{int} in (mg/g $min^{1/2}$) is the intra-particle diffusion constant, C: constant

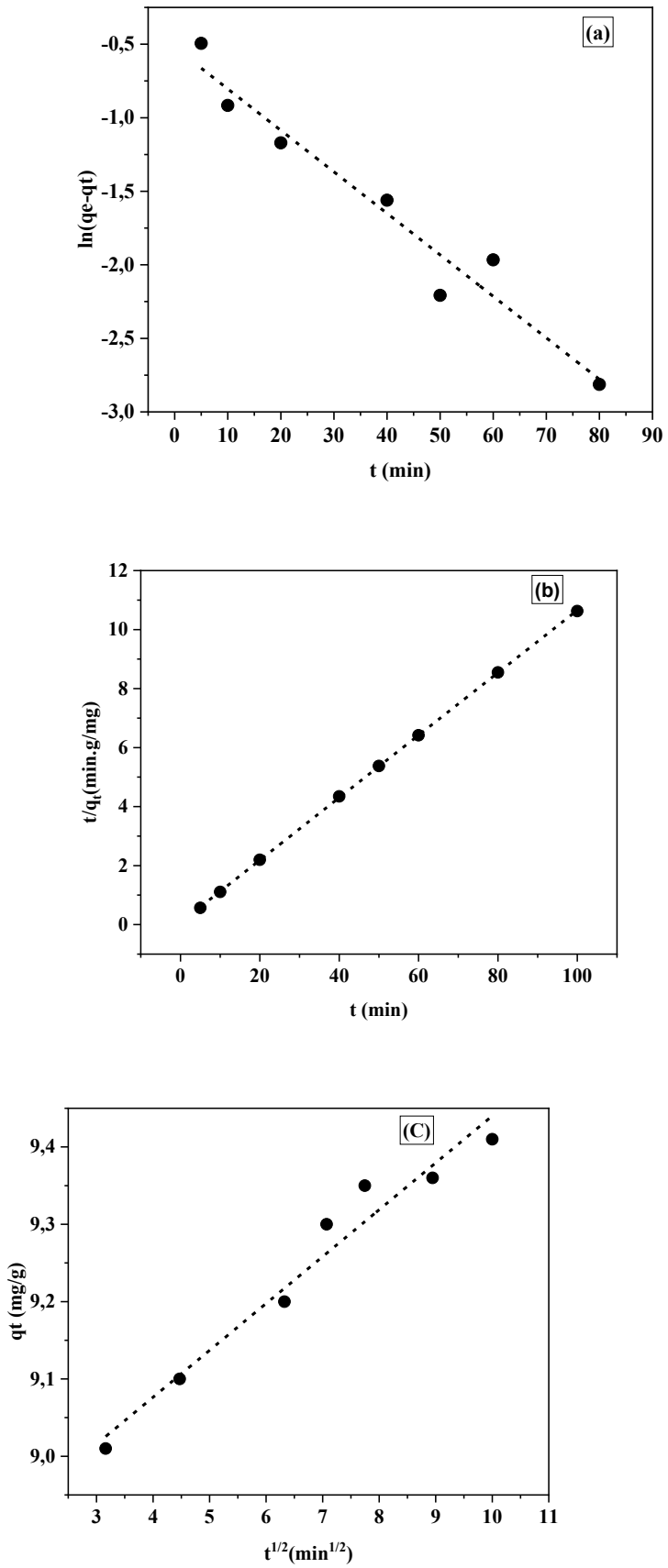

Fig 11. Models for the adsorption of MB onto *Acacia raddiana* biomass : **a** Pseudo-first-order, **b** Pseudo-second-order and **c** Intraparticle diffusion

Table 3. Kinetic Parameters for the Adsorption of MB onto *Acacia raddiana* biomass

Model	Parameter	Values	R^2
First order kinetics	K_1 (min^{-1})	0.064	0.94
	qe (mg/g)	0.593	
Second order kinetics	K_2 (g/mg min)	0.163	0.99
	qe (mg/g)	9.445	
Intraparticle diffusion	Kint ($mg/g.min^{1/2}$)	8.83	0.96
	C	0.06	

Based on parameters obtained after linear adjustments as showed in Table 3, a considera bly higher coefficient of correlation (R^2= 0.99) was associated with the pseudo- second-order kinetics. Therefore, it is clear that a more successful biosorption is represented by the pseudo-second-order model. Additionally, qe= 9.445 mg/g, the close consistency between experimental and predicted equilibrium adsorption capacities indicates that distinct surface sites and binding locus on the adsorbent outer layer are fundamentally participant in the sorption system. A faster adsorption rate is implied by the pseudo second-order model's higher rate constant (K_2 = 0.163 g/mg min) than by the pseudo-first-order model's (K_1 = 0.064 min^{-1}).

Table 4: Comparison of adsorption capacities of various naturel adsorbents methylene bleu removal

Adsorbent	**Adsorption Capacities qe (mg/g)**	**Reference**
rice husk	25.50	(Quansah et al., **2020**)
Prunus spinosa L	59.59	(Onuk et al., **2025**)
Mango peel	277.8	(Jawad et al., **2017**)
Acacia	133.0	(Chawraba et al., **2025**)
Lemon leaf powder	8	(Babu et al., **2023**)
Raw pine leaf biomass	36.88	(Sen, **2023**)
Cordia africana leaf	6.25	(Teweldebrihan et al., **2025**)
Acacia raddiana bark	9.128	This study

4. CONCLUSION

The intention of this study is to show how the MB dye's adsorption capability is affected by the inherent adsorption qualities of *Acacia raddiana* bark biomass. Multiple variables, including pH, starting dye concentration, contact time, temperature, and adsorbent mass, were examined for their impacts. After 100 minutes of contact, the maximum removal quantity of 9.128 mg/g is reached. The optimal pH for adsorption is 10. An R^2 value of 0.99 indicates that the Langmuir isotherm offers an accurate approximation of the experimental results. This suggests homogenous interactions and demonstrates that the adsorbent occupies the single layer of colorant. A positive ΔS denotes increased molecular disorder at the interface between the adsorbent and the MB solution during adsorption onto *Acacia raddiana* bark, a negative ΔG denotes spontaneous adsorption, and a positive ΔH denotes an endothermic process, according to the obtained thermodynamic parameters. A kinetic study confirmed that the system fits into a pseudo-second-order model, with a significant correlation between the anticipated and actual adsorption capabilities. These results highlight the possibility of biomass from *Acacia raddiana* bark as a sustainable and efficient material for treating MB dye-contaminated industrial wastewater.

5. REFERENCES

1. Abdel Azim E, Samy M, Hanafy M, Mahanna H. (2024). Novel mint-stalks derived biochar for the adsorption of methylene blue dye: Effect of operating parameters, adsorption mechanism, kinetics, isotherms, and thermodynamics. *J Environ Manage* 357(1):120738.
2. Afolalu SA, Ikumapayi OM, Ogedengbe TS. (2022). Waste pollution, wastewater and effluent treatment methods – An overview. *Mater Today Proc* 62:3282-3288.
3. Al-Harby NF, Albahly EF, Mohamed NA. (2021). Kinetics, Isotherm and Thermodynamic Studies for Efficient Adsorption of Congo Red Dye from Aqueous Solution onto Novel Cyanoguanidine-Modified Chitosan Adsorbent. *Polymers* 13(1):4446.
4. Asgari G, Seid-Mohammadi A, Rahmani A, Shokoohi R, Abdipour H. (2024). Concurrent elimination of arsenic and nitrate from aqueous environments through a novel nanocomposite: Fe3O4-ZIF8@eggshell membrane matrix. *J Mol Liq* 396(1):124037.

5. Ashraf M, Rehman R, Hatshan MR, Bathula C, Dar A, Akram M. (2024). Process Modeling of Methylene Blue Dye Adsorptive Removal by Physio-chemically treated Cicer arietinum Husk for Effective Wastewater Treatment by Green Chemistry. *Water Air Soil Pollut* 235(1):166.
6. Babu SB and Priyanka SV. (2023). Removal of malachite green dye from aqueous solution using lemon leaf powder as an adsorbent. *J Solid Waste Technol Manag* 49(2):141–151.
7. Bhavyasree PG and Xavier TS. (2021). Adsorption studies of methylene blue, coomassie brilliant blue, and congo red dyes onto CuO/C nanocomposites synthesized via vitex negundo linn leaf extract. *Curr Res Green Sustain Chem* 4(1):100161.
 Bih NL, Rwiza MJ, Ripanda AS, Mahamat AA, Machunda RL, Choi JW. (2025). Adsorption of phenol and methylene blue contaminants onto high-performance catalytic activated carbon from biomass residues. *Heliyon* 11(1):e30134.
8. Cai H, Niu Y, Guan T, Zhang Y, Ma Z. (2024). Removal of metronidazole using a novel ZnO–CoFe2O4@Biochar heterostructure composite in an intimately coupled photocatalysis and biodegradation system under visible light. *J Environ Manage* 364(1):121431.
9. Chawraba K, El Malti W, Akil A, M Hamieh, M Hammoud, D Patra, J Toufaily, A Hijazi. (2025). Optimized Adsorption of Dyes and Antibiotics onto Natural Acacia Ataxacantha for Water Treatment. *ACS Omega* 10:24847-24861.
10. Cheruiyot GK, Wanyonyi WC, Kiplimo JJ, Maina EN. (2019). Adsorption of toxic crystal violet dye using coffee husks: Equilibrium, kinetics and thermodynamics study. *Sci Afr* 5(1):1–11.
11. De Oliveira TF, De Souza CP, Lopes-Moriyama AL, Pereira da Silva ML. (2023). In situ modification of MCM-41 using niobium and tantalum mixed oxide from columbite processing for methylene blue adsorption: characterization, kinetic, isotherm, thermodynamic and mechanism study. *Mater Chem Phys* 294(1):127011.
12. Dimbo D, Abewaa M, Adino E, A Mengistu, T Takele, A Oro, M Rangaraju. (2024). Methylene blue adsorption from aqueous solution using activated carbon of spathodea campanulata. *Results Eng* 21(1):101910.
13. Dutta S, Gupta B, Srivastava SK. (2021). Recent advances on the removal of dyes from wastewater using various adsorbents: a critical review. *Anal Methods* 13:4497-4531.
14. El-Nemr MA, Yılmaz M, Ragab S, Hassaan MA. (2023). Isotherm and kinetic studies of acid yellow 11 dye adsorption from wastewater using Pisum Sativum peels microporous activated carbon. *Sci Rep* 13:4268.
15. Ewis D, Ba-Abbad MM, Benamor A, Mahmud N, Nasser M, El-Naas M, Mohammad AW. (2022). Adsorption of 4-Nitrophenol onto Iron Oxide Bentonite Nanocomposite: Process Optimization, Kinetics, Isotherms and Mechanism. *Int J Environ Res* 16(1):1–13.
16. Ezzati R, Ezzati S, Azizi M. (2024). Exact solution of the Langmuir rate equation: new insights into pseudo-first-order and pseudo-second-order kinetics models for adsorption. *Vacuum* 220(1):112790.
 Farghali RA, Sobhi M, Gaber SE, Ibrahim H, Elshehy EA. (2020). Adsorption of Organochlorine Pesticides on Modified Porous Al30/ Bentonite: Kinetic and Thermodynamic Studies. *Arab J Chem* 13(1):6730-6740.
 Gamboa DMP, Abatal M, Lima E, Franseschi FA, Ucán CA, Tariq R, Elías MAR, Vargas J. (2024). Sorption behavior of azo dye congo red onto activated biochar from haematoxylum campechianum waste: gradient boosting machine learning-assisted Bayesian optimization for improved adsorption process. *Int J Mol Sci* 25(9):4771.
 Haleem A, Shafiq A, Chen SQ, Nazar M. (2023). A Comprehensive Review on Adsorption, Photocatalytic and Chemical Degradation of Dyes and Nitro-Compounds over Different Kinds of Porous and Composite Materials. *Molecules* 28(1):1081.
17. Hamzah HT, Sridevi V, Surya DV, Palla S, Yadav A, Rao PV. (2023). Conventional and microwaveassisted acid pretreatment of tea waste powder: Analysis of functional groups using FTIR. *Environ Sci Pollut Res* 1(1):1–10.
18. Jaramillo-Fierro X and Cuenca G. (2024). Theoretical and Experimental Analysis of Hydroxyl and Epoxy Group Effects on Graphene Oxide Properties. *Nanomaterials* 14(1):8.
19. Javed I, Hanif MA, Rashid U, Nadeem F, Alharthi FA, Kazerooni EA. (2022). Enhancing functionalities in nanocomposites for effective dye removal from wastewater: isothermal, kinetic and thermodynamic aspects. *Water* 14(1):2600.
20. Jawad AH, Mamat NFH, Abdullah MF, Ismail K. (2017). Adsorption of methylene blue onto acid-treated mango peels: kinetic, equilibrium and thermodynamic study. *Desalin Water Treat* 59:210–219.
21. Kassahun E, Fito J, Tibebu S, Nkambule TTI. (2022). The application of the activated carbon from Cordia Africana leaves for adsorption of chromium (III) from an aqueous solution. *J Chem* 2022:1–11.
22. Khairnar SD, Shirsath DS, Patil PS, Shrivastava VS. (2020). Adsorptive and photocatalytic removal of carcinogenic methylene blue dye by SnO2 nanorods: an equilibrium, kinetic and thermodynamics exploration. *SN Appl Sci* 2(1):1–12.
23. Khan SA, Ponce P, Yu Z. (2022). Environmental technology and wastewater treatment: Strategies to achieve environmental sustainability. *Chemosphere* 286(1):131532.
24. Kifuani KM, Kifuani Kia Mayeko A, Noki P**.** (2018). Adsorption of a basic dye, methylene blue, in aqueous solution on a bioadsorbent derived from agricultural waste from Cucumeropsis mannii Naudin. *Int J Biol Chem Sci* 12(1):558-575.
25. Kucuk I. (2024). Effect of KOH- and NaOH-modified fly ash on the adsorption of methylene blue and crystal violet dyes: a Box-Behnken design study. *Int J Environ Anal Chem* 1(1):1–20.
26. Kumari S, Agarwal S, Kumar M, Sharma P, Kumar A, Hashem A, Alotaibi NH, Abd-Allah EF. (2025). An exploration of RSM, ANN, and ANFIS models for methylene blue dye adsorption using Oryza sativa straw biomass: a comparative approach. *Sci Rep* 15(1):2979.
27. Kumari S, Chowdhry J, Sharma P, Agarwal S, Garg MC. (2023). Integrating artificial neural networks and response surface methodology for predictive modeling and mechanistic insights into the detoxification of hazardous MB and CV dyes using Saccharum officinarum L. biomass. *Chemosphere* 344(1):140262.
28. Kumari S, Singh S, Lo SL, Sharma P, Agarwal S, Garg MC. (2025). Machine learning and modelling approach for removing methylene blue from aqueous solutions: Optimization, kinetics and thermodynamics studies. *J Taiwan Inst Chem Eng* 16(1):105361.
29. Manera C, Tonello AP, Perondi D, Godinho M. (2019). Adsorption of leather dyes on activated carbon from leather shaving wastes: Kinetics, Equilibrium and Thermodynamics Studies. *Environ Technol* 40(1):2756-2768.
30. Mohamed F, Shaban M, Zaki SK, Abd-Elsamie MS, Sayed R, Zayed M, Khalid N, Saad S. (2022). Activated carbon derived from sugarcane and modified with natural zeolite for efficient adsorption of methylene blue dye: experimentally and theoretically approaches. *Sci Rep* 12(1):18031.

31. Montoya-Escobar N, D Ospina-Acero D, Velásquez-Cock JA, C Gómez-Hoyos C. (2022). Use of fourier series in X-ray diffraction (XRD) analysis and fourier-transform infrared spectroscopy (FTIR) for estimation of crystallinity in cellulose from different sources. *Polymers* 14(11):2150.
32. Khatun MA, Alam MJ, Chowdhury S, Khan MAR. (2023). Adsorption of methylene blue on papaya bark fiber: Equilibrium, isotherm and kinetic perspectives. *Results Eng* 17(1):2590-1230.
33. Nursiah C, Desvita H, Elviani E, Farida N, Muslim A, Rosnelly CM, Mariana M. (2023). Adsorbent characterization from cocoa shell pyrolysis (Theobroma cacao L) and its application in mercury ion reduction. *J Ecol Eng* 24:366–375.
34. Onuk EB and Isik B. (2025). Adsorptive removal of toxic methylene blue and crystal violet dyes from aqueous solutions using Prunus spinosa: isotherm, kinetic, thermodynamic, and error analysis. *Biomass Convers Biorefin* 15(1):239–254.
35. Periyasamy AP. (2024). Recent advances in the remediation of textile-dye-containing wastewater: prioritizing human health and sustainable wastewater treatment. *Sustainability* 6(1):495.
36. Quansah JO, Hlaing T, Lyonga FN, Kyi PP, Hong SH, Lee CG, Park SJ. (2020). Nascent Rice Husk as an Adsorbent for Removing Cationic Dyes from Textile Wastewater. *Appl Sci* 10(10):3437.
37. Rana S, Bhadauria P, Kumar V. (2021). Methylene Blue Dye Removal from Wastewater Using Ailanthus Excelsa Roxb as Adsorbent. *Water Conserv Sci Eng* 2021;6(1):1–9.
38. Salameh FF, Ba-Abbad MM, Hameed BH. (2025). Sustainable Detoxification of Methylene Blue in Wastewater via Tea Residue Adsorption: Optimization and Kinetics. *Water Air Soil Pollut* 236(1):123.
39. Sarioz N, Isik B, Cakar F, Cankurtaran O. (2024). Valorization of the performance of novel and natural sodium alginate/pectin/Portulaca oleracea L. ternary composites in the adsorption of toxic methylene blue dye from the aquatic environment. *Int J Biol Macromol* 282:136867.
40. Sarojini G, Babu SV, Rajamohan N, Rajasimman M, Pugazhendhi A. (2022).Application of a polymer-magnetic-algae based nano-composite for the removal of methylene blue-characterization, parametric and kinetic studies. Environ Pollut 292(1):118376.
41. Sen N, Shefa NR, Reza K, Shawon SMAZ, Rahman MW. (2024). Adsorption of crystal violet dye from synthetic wastewater by ball-milled royal palm leaf sheath. Sci Rep 14(1):14878.
42. Sen TK. (2023). Adsorptive removal of dye (methylene blue) organic pollutant from water by pine tree leaf biomass adsorbent. Processes 11:1877.
43. Shanableh A, Shafiquzzaman M, Osman H, Al-Ansari N. (2023). Isotherms, kinetics and thermodynamic mechanism of methylene blue dye adsorption on synthesized activated carbon. J Water Manag 45:123-145.
44. Singh M, Pahal V, Ahuja D. (2020). Isolation and characterization of microfibrillated cellulose and nanofibrillated cellulose with 'biomechanical hotspots.' Carbohydr Polym 234:115827.
45. Teweldebrihan MD, Gnaro MA, Dinka MO. (2025). Adsorptive removal of malachite green dye from aqueous solution using Cordia africana leaf as biosorbent. Model Earth Syst Environ 11:86.
46. Vigdorowitsch M, Pchelintsev A, Tsygankova L, Tanygina E. (2021). Freundlich isotherm: An adsorption model complete framework. Appl Sci 11(1):8078.
47. Wang L, Shi C, Pan L, Zhang X, Zou JJ. (2020). Rational design, synthesis, adsorption principles and applications of metal oxide adsorbents: a review. *Nanoscale* 12(8):4790-4815.
48. Yang L, Bao L, Zhong Y, Hao C, Chen J, Wu J, Wang X. (2024). Fabrication of in situ metal-organic framework grown on sodium lignosulphonate hydrogel for removal of Pb^{2+}, methylene blue and crystal violet from aqueous solution. *J Clean Prod* 434(1):139831.